# Bioactive Segetane, Ingenane, and Jatrophane Diterpenes from *Euphorbia taurinensis*

**Authors**
Dóra Rédei[1], Norbert Kúsz[1], Gréta Sátori[1], Annamária Kincses[2], Gabriella Spengler[2], Katalin Burián[2], Zoltán Barina[3], Judit Hohmann[1,4]

**Affiliations**
1 Department of Pharmacognosy, University of Szeged, Szeged, Hungary
2 Department of Medical Microbiology and Immunobiology, University of Szeged, Szeged, Hungary
3 Department of Botany, Hungarian Natural History Museum, Budapest, Hungary
4 Interdisciplinary Centre of Natural Products, University of Szeged, Szeged, Hungary

**Correspondence**
Prof. Dr. Judit Hohmann
Department of Pharmacognosy, University of Szeged
Eötvös u. 6, 6720 Szeged, Hungary
Phone: + 36 62 54 64 53, Fax: + 36 62 54 57 04
hohmann@pharm.u-szeged.hu

⊕ Supporting information available online at
http://www.thieme-connect.de/products

**ABSTRACT**

A novel segetane (**1**) and jatrophane diterpene (**2**), together with five known diterpenoids possessing segetane (**3**), jatrophane (**4**), and ingenane skeletons (**5–7**), were isolated from the methanol extract of *Euphorbia taurinensis* All. The structure elucidation of the compounds was performed by means of extensive spectroscopic analysis, including HRESIMS and 1D (${}^1$H, *J*-modulated spin-echo carbon experiment) and 2D (HSQC, HMBC, COSY, NOESY) NMR experiments. The multidrug resistance reversing and cytotoxic effects of five diterpenes (**1, 4–7**) were studied on the L5178 mouse lymphoma cell line using rhodamine 123 accumulation and the MTT cell viability assay. Segetane and jatrophane diterpenes had no cytotoxic activity on the sensitive parent and multidrug resistance cells, while ingenane diterpenes showed a cytotoxic effect on both cell lines. Ingenanes **6** and **7** and segetane **1** demonstrated the remarkable multidrug resistance modulating effect at 20 µM.

## Introduction

*Euphorbiaceae* is an enormous and incredibly diverse family of flowering plants, comprising approximately 6600 species in 228 genera [1]. Diterpenes are characteristic secondary metabolites of spurge species, which are responsible for the caustic, mucosa irritant, proinflammatory, and carcinogenic features of the milky latex. The great variability of diterpene skeletons and acylation patterns are accompanied by multiple interactions with living organisms, some of which are potentially exploitable in the treatment of different diseases. Tigliane, daphnane, and ingenane diterpenes, referred to collectively as phorboids, have received particular attention due to their remarkable pharmacological proper-

ties [2, 3]. EBC-46 (tigliol tiglate) is a novel activator of a specific subset of enzymes with a promising anticancer effect. Local application of the compound causes rapid tumor ablation through hemorrhagic necrosis and tumor vasculatory destruction, supporting its use in cutaneous malignancies [4]. Prostratin, belonging to the tigliane group, reactivates latent HIV-1 reservoirs in infected CD4+ cells via protein kinase C-dependent nuclear factor-kappa B activation, and therefore promotes complete virus eradication as an adjuvant intervention of antiretroviral therapy [5]. Gnidimacrin, a daphanane diterpene isolated from *Stellera chamaejasme* L., was recently reported to significantly decrease latent HIV-1 DNA levels and frequency of latently infected cells in human *ex vivo* models [6]. Ingenol 3-angelate is the active ingredient of

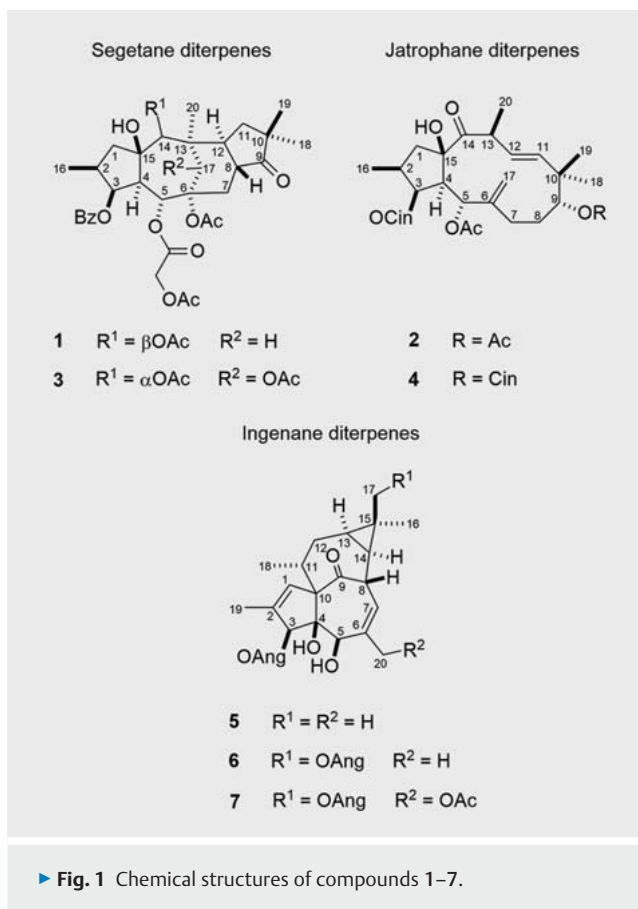Rédei D et al. Bioactive Segetane, Ingenane, … Planta Med 2018; 84: 729–735

729

**ABBREVIATIONS**

| | |
|---|---|
| ABCB1 | ATP-binding cassette subfamily B member 1 |
| EMA | European Medicines Agency |
| FAR | fluorescence activity ratio |
| FDA | Food and Drug Administration |
| HSQC | heteronuclear single quantum correlation |
| JMOD | *J*-modulated spin-echo carbon experiment |
| MDR | multidrug resistance |
| NP-HPLC | normal phase high performance liquid chromatography |
| OD | optical density |
| PAR | parental cells |
| R123 | rhodamine 123 |
| RP-PLC | reversed-phase preparative layer chromatogaphy |
| TRPV-1 | transient receptor potential cation channel sub-family V member 1 |



▶ **Fig. 1** Chemical structures of compounds **1–7**.

the EMA- and FDA-approved topical preparation Picato for the treatment of the precancerous skin disorder actinic keratosis [7]. Resiniferatoxin is an ultrapotent capsaicin analogue that selectively binds to the TRPV-1 vanilloid receptors of afferent neurons, and interrupts the transmission of nociceptive signals to the brain [8]. Resiniferatoxin is currently undergoing clinical phase I and II trials evaluating the efficacy and safety of its intrathecal and epidural administrations in alleviating intractable pain in patients with advanced cancer [9, 10]. Therapeutic relevance of jatrophane diterpenes with noteworthy P-glycoprotein modulatory, cytotoxic, antiproliferative, antiplasmodial, and antiviral activities was also demonstrated by several studies [11–16]. The development of MDR to chemotherapy is a major obstacle regarding the effective treatment of many malignancies. It has been described that one of the most common mechanisms of cancer MDR is the overexpression of various efflux pumps (ABCB1/P-glycoprotein, ABCC1/MRP-1, ABCG2/BCRP), which are membrane-associated proteins that can recognize and extrude various anticancer drugs out of the cells. Modulation of the most studied ABCB1 efflux pump using novel, plant-derived efflux pump inhibitors can be a promising approach to overcome MDR in cancer. It has been described that diterpenes from *Euphorbia* species have been shown to have potential MDR-reversing activities [17–19].

*Euphorbia taurinensis* All. is a glabrous annual plant distributed across southern and central regions of Europe [20]. As a continuation of our search for bioactive natural products from the genus *Euphorbia*, we present here the first phytochemical investigation of *E. taurinensis*. Hereby we describe the isolation and structure elucidation of segetane (**1**, **3**), jatrophane (**2**, **4**), and ingenane (**5–7**) diterpenes, and evaluation of the cytotoxic and MDR-reversing activity of the isolated compounds.

## Results and Discussion

A fresh whole plant of *E. taurinensis* All. was exhaustively extracted with methanol at room temperature, then partitioned between $CHCl_3$ and a mixture of MeOH-water. The $CHCl_3$-soluble phase was fractionated on an open polyamide column. Fractions eluted with MeOH-water 4:1 and 3:2 were separated by various chromatographic methods, including vacuum liquid chromatography, preparative TLC, and HPLC to furnish seven pure compounds possessing segetane (**1**, **3**), jatrophane (**2**, **4**), and ingenane (**5–7**) skeletons (▶ **Fig. 1**). Structure determination was carried out by means of one- (^{1}H, JMOD) and two-dimensional (HSQC, HMBC, ^{1}H-^{1}H COSY, NOESY) NMR spectroscopic methods and HR-ESIMS measurements.

Compound **1** was obtained as a white amorphous powder. It has the molecular formula of $C_{35}H_{44}O_{12}$, compatible with the pseudomolecular ion peak at $m/z$ 674.3180 $[M + NH_4]^+$ (calcd. for $C_{35}H_{48}O_{12}N$ 674.3177, $\Delta = -0.3$ mmu) and 679.2729 $[M + Na]^+$ (calcd. for $C_{35}H_{44}O_{12}Na$ 679.2731, $\Delta = +0.2$ mmu) in the HRESIMS spectrum. From the ^{1}H and JMOD spectra, three esters were easily identified as one benzoyl [$\delta_H$ 7.84 d (2H), 7.58 t (1H), 7.46 t (2H); $\delta_C$ 166.0, 133.5, 129.6, 129.4, and 128.9] and two acetyl [$\delta_H$ 2.15 s (3H), 2.07 s (3H); $\delta_C$ 170.5, 170.9, 21.2, and 21.9)] groups (▶ **Table 1**). The remaining two ester carbonyls ($\delta_C$ 170.2, 167.0), an acetyl methyl ($\delta_H$ 2.08 s; $\delta_C$ 20.6), and an isolated oxymethylene ($\delta_H$ 4.58 d, 4.48 d; $\delta_C$ 60.6) confirmed the presence of an uncommon acetoxyacetate moiety. Apart from the esterifying acids, the JMOD spectrum displayed 20 carbon resonances attributed to a diterpene skeleton. Investigation of the HSQC spectrum revealed that four methyls, four methylenes, and seven methines (including three oxymethines) are involved in the

**730**

Rédei D et al. Bioactive Segetane, Ingenane, … Planta Med 2018; 84: 729–735

▶ **Table 1** ¹H and ¹³C NMR data of compounds **1** and **2** [$\delta$ ppm ($J$ = Hz), CDCl₃, 500 MHz (¹H), and 125 MHz (¹³C)].

| | **1** | | **2** | |
|---|---|---|---|---|
| | $\delta_H$ | $\delta_C$ | $\delta_H$ | $\delta_C$ |
| 1a | 2.37 dd (15.1; 9.3) | 50.5 | 2.38 dd (13.8; 8.6) | 46.9 |
| 1b | 1.54 dd (15.1; 11.6) | | 1.84 m | |
| 2 | 2.07 m | 37.2 | 2.28 m | 38.6 |
| 3 | 5.79 br s | 81.1 | 5.73 br s | 77.9 |
| 4 | 3.28 dd (11.5; 3.1) | 48.4 | 2.76 dd (10.1; 3.2) | 50.5 |
| 5 | 5.29 d (11.5) | 70.4 | 5.69 (10.1) | 73.5 |
| 6 | – | 82.4 | – | 142.8 |
| 7a | 2.57 br d (12.4) | 38.2 | 2.18 m | 27.1 |
| 7b | 1.28 t (12.5) | | 1.62 m | |
| 8 | 3.64 ddd (15.1; 12.4; 3.1) | 47.0 | 1.46 m (2H) | 27.7 |
| 9 | – | 220.1 | 4.36 d (8.3) | 79.7 |
| 10 | – | 45.8 | – | 41.2 |
| 11a | 1.92 br d (12.1) | 36.7 | 5.44 d (16.0) | 137.1 |
| 11b | 1.85 dd (11.5; 5.4) | | | |
| 12 | 1.50 dd (15.1; 5.4) | 48.2 | 5.42 d (16.0) | 129.2 |
| 13 | – | 41.3 | 3.40 m | 44.4 |
| 14 | 5.12 s | 75.8 | – | 213.0 |
| 15 | – | 83.1 | – | 84.8 |
| 16 | 0.93 d (6.7) | 14.4 | 1.06 d (6.2) | 14.2 |
| 17a | 3.54 d (14.5) | 39.0 | 5.14 s | 114.8 |
| 17b | 1.05 d (14.5) | | 4.69 s | |
| 18 | 1.03 s | 24.9 | 1.04 s | 27.5 |
| 19 | 1.12 s | 26.7 | 1.05 s | 18.1 |
| 20 | 1.03 s | 30.8 | 1.33 d (6.4) | 21.8 |
| 15-OH | 2.44 s | – | 4.30 s | – |
| 3-OBz | | | | |
| 1′ | – | 166.0 | | |
| 2′ | – | 129.6 | | |
| 3′, 7′ | 7.84 d (7.5) (2H) | 129.4 | | |
| 4′, 6′ | 7.46 t (7.6) (2H) | 128.9 | | |
| 5′ | 7.58 t (7.4) | 133.5 | | |
| 3-OCin | | | | |
| 1′ | | | – | 167.0 |
| 2′ | | | 6.48 d (15.9) | 117.8 |
| 3′ | | | 7.73 d (15.9) | 145.7 |
| 4′ | | | – | 134.5 |
| 5′, 9′ | | | 7.55 m (2H) | 128.5 |
| 6′, 8′ | | | 7.37 m (2H) | 128.9 |
| 7′ | | | 7.37 m | 130.4 |
| 5-OAcAc | | | | |
| C=O | – | 167.0 | | |
| CH₂-O- | 4.58 d (15.9) | 60.6 | | |
| | 4.48 d (15.9) | | | |
| C=O | – | 170.2 | | |
| CH₃ | 2.08 s | 20.6 | | |

*continued*

▶ **Table 1** *Continued*

| | 1 | | 2 | |
|---|---|---|---|---|
| | $\delta_H$ | $\delta_C$ | $\delta_H$ | $\delta_C$ |
| 5-OAc | | | – | 169.3 |
| | | | 1.93 s | 21.2 |
| 6-OAc | – | 170.9 | | |
| | 2.07 s | 21.9 | | |
| 9-OAc | | | – | 170.9 |
| | | | 2.05 s | 21.2 |
| 14-OAc | – | 170.5 | | |
| | 2.15 s | 21.2 | | |

formation of the parent system. Furthermore, five signals with absent HSQC cross-peaks were classified as one keto ($\delta_C$ 220.1), two oxygen attached ($\delta_C$ 83.1, 82.4), and two alkylic ($\delta_C$ 41.3, 45.8) quaternary carbons in accordance with their chemical shifts. From the molecular formula, 14 degrees of unsaturation was deduced, which (excluding the benzene ring and the carbonyl atoms) required the presence of a tetracyclic framework. The $^1$H-$^1$H COSY spectrum provided three sequences of correlated protons: –CH$_2$–CH(CH$_3$)–CH(OR)–CH–CH(OR)– ($\delta_H$ 2.37 dd, 1.54 dd, 2.07 m, 0.93 d, 5.79 br s, 3.28 dd, 5.29, d) (A), –CH$_2$–CH–CH–CH$_2$– ($\delta_H$ 2.57 br d, 1.28 t, 3.64 ddd, 1.50 dd, 1.92 br d, 1.85 dd) (B), and a geminal proton pair –CH$_2$– ($\delta_H$ 3.54 d, 1.05 d) (C). Detailed analysis of the HMBC spectrum established the connectivities of partial structures A–C separated by quaternary carbons. $^2J_{C,H}$ and $^3J_{C,H}$ couplings between H-1b, H-3, H-5, H-14, and 15-OH with C-15 ($\delta_C$ 83.1) suggested that fragment A forms a methyl and hydroxyl-substituted five-membered ring characteristic to Euphorbiaceae diterpenes. Detected long-range correlations of H-4, H-5, H-7a/b, and H-17a/b with C-6 ($\delta_C$ 82.4), as well as H-11a, H-12, H-14, H-17a/b, and H-20 with C-13 ($\delta_C$ 41.3) led to the conclusion that spin systems A–C and a tertiary methine (C-14) are incorporated in a bicyclo[4.3.1]decane ring system occurring primarily in segetane diterpenes. Selected $^1$H-$^1$H COSY and HMBC (C → H) correlations for **1** are presented in ▶ **Fig. 2**. HMBC cross-peaks between H-11a/b, H-18, H-19, and C-10 ($\delta_C$ 45.8), together with H-7b, H-8, H-11b, H-18, H-19, and C-9 ($\delta_C$ 220.1), proposed subunit B and two tertiary methyls to compose an additonal cyclopentane ring and located the keto group on the terpenoid scaffold. The position of the ester groups were determined via $^3J_{C,H}$ interactions of oxymethine protons H-3, H-5, H-14 with carbonyls at $\delta_C$ 166.0 (benzoyl), 167.0 (acetoxyacetyl), and 170.5 (acetyl), respectively. The acyl residue at $\delta_H$ 2.07 exhibited a weak four-bond correlation with C-6 ($\delta_C$ 82.4), therefore, it must be situated on C-6. The relative configuration of the stereogenic centers were assessed by means of a NOESY experiment. Conventionally, H-4 at the ring juction was chosen as the initial $\alpha$ reference point. NOE cross-peaks between hydrogen pairs H-4/H-2 and H-4/H-17a indicated the $\beta$ position of the C-16 methyl, and revealed the $\alpha$ configuration of the C-17 bridge. The $\beta$ position of the C-3 benzoyl substituent was proved by the NOESY correlation between benzo-
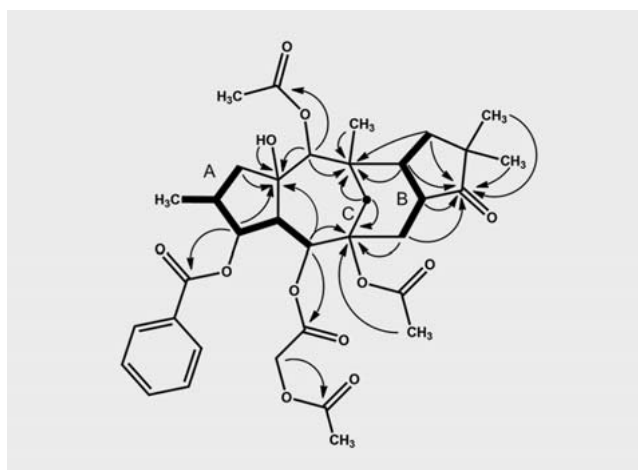


▶ **Fig. 2** Key COSY (–) and HMBC (H → C) correlations of compound **1**.

yl H-3′,7′ and 15-OH. Diagnostic Overhauser effects of H-5 with H-7$\beta$, H-8, and 15-OH determined the $\alpha$ orientation of the acetoxyacetate unit attached to C-5, while NOEs of 15-OH/H-1$\beta$, H-14/H-1$\alpha$, and H-14/H-20 dictated the rare $\beta$ orientation of an acetyl group on C-14 [21]. The large value of vicinal coupling $J_{8,12}$ = 15.1 Hz demonstrated the rigid antiperiplanar relationship of the corresponding hydrogens [22]. Geminal protons attached to C-11 were distinguished via H-11a/H-19, H-11b/H-18, and H-12/H-18 interactions. The above stereochemical findings were in good agreement with a minimum energy conformation generated by molecular dinamics calculations as depicted in ▶ **Fig. 3**.

Compound **2** was isolated as a white amorphous powder. Its HRMS spectrum exhibited a sodium adduct ion peak at *m/z* 589.2773 [M + Na]$^+$ (calcd. for $C_{33}H_{42}O_8Na$ 589.2777, $\Delta$ = + 0.4 mmu), assigning the molecular formula of $C_{33}H_{42}O_8$. Comparison of $^1$H-NMR data (▶ **Table 1**) with the known jatrophane diterpene **4** indicated the same polyol core, however, the absent resonances of a cinnamoyl acid, an additional acetyl singlet at $\delta_H$ 2.05 ppm, and the slightly downfield shifted H-9 ($\delta_H$ 4.36 d) suggested a different esterification pattern of C-9. This deduction

732

Rédei D et al. Bioactive Segetane, Ingenane, … Planta Med 2018; 84: 729–735
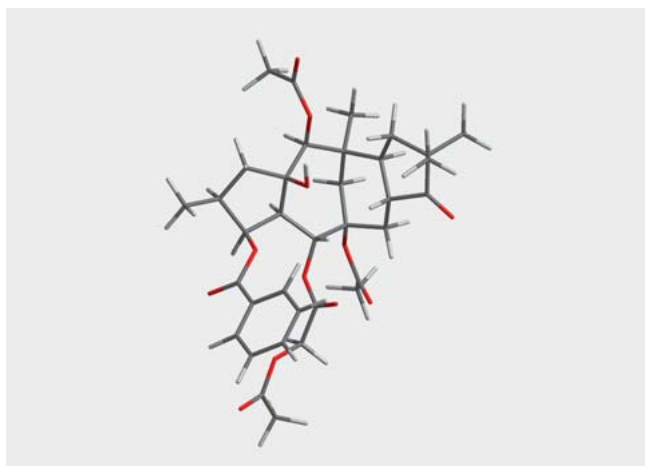
▶ **Fig. 3** Calculated molecular structure of compound **1**.

▶ **Table 2** Cytotoxic activity of compounds **1** and **4–7** on parent and multidrug-resistant mouse T-lymphoma cells.

| Com-pound | Parent mouse T-lymphoma cells | | MDR mouse T-lymphoma cells | |
|---|---|---|---|---|
| | IC$_{50}$ [µM] | CI | IC$_{50}$ [µM] | CI |
| 1 | > 100 | – | > 100 | – |
| 4 | > 100 | – | > 100 | – |
| 5 | > 100 | – | > 100 | – |
| 6 | 53.35 | 51.34–55.36 | 59.83 | 58.25–61.41 |
| 7 | 82.47 | 80.38–84.56 | 62.81 | 61.65–63.97 |
| Doxo-rubicin | 0.7 | 0.42–0.98 | 2.14 | 1.76–2.52 |

was further substantiated by observed $^2J_{C,H}$ and $^3J_{C,H}$ heteronuclear couplings between H-9, 9-OAc methyl, and the carbonyl atom at $\delta_C$ 170.9. Series of NOE correlations H-3/H-2, H-4/H-3, H-4/H-13, H-11/H-13, as well as H-5/15-OH, H-9/H-12, H-9/H-19, and H-12/H-20 permit the same stereochemistry of chiral carbons as Jakupovic et al. reported for compound **4**. NOESY cross-peak between H-8/H-17b together with the large coupling constant between C-4 and C-5 ($J_{4,5}$ = 10.1 Hz) indicates that the C-17 methylene is not parallel with the mean plane of the 12-membered macrocycle, therefore, compound **2** has an *endo*-type conformation [22, 23].
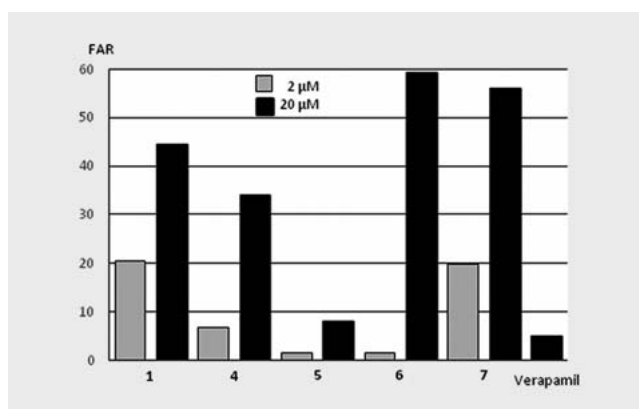
Compounds **3–7** were identified as known metabolites of Euphorbiaceae species. Compound **3** was found to be identical with paralinone A, isolated from *Euphorbia paralias* and *Euphorbia segetalis* [22, 24]. Compound **4** was proven to be 5-acetoxy-3,9-dicinnamoyloxy-15-hydroxy-14-oxo-jatropha-6(17),11*E*-diene, previously described only from *E. segetalis* [22]. $^1$H and $^{13}$C spectral data of **5–7** perfectly superimposed with literature values of 3-*O*-angeloyl-20-deoxyingenol, 3-*O*-angeloyl-17-angeloyloxy-20-deoxyingenol, and 20-*O*-acetyl-3-*O*-angeloyl-17-angeloyloxyingenol, respectively [22, 25, 26].

Segetanes represent a peculiar and rare class of diterpenes, only 12 compounds have been described from *E. paralias, E. segetalis, Euphorbia portlandica*, and *Euphorbia peplus*, to date [21, 22, 24, 26–29]. According to an earlier classification, *E. taurinensis* and *E. peplus* were considered to be members of section *Cymatospermum* (Prokh.) Prokh., while *E. paralias, E. segetalis*, and *E. portlandica* belonged to the section *Paralias* Dumort [20]. New phylogenetic studies suggest that *E. taurinensis, E. paralias, E. segetalis*, and *E. portlandica* are members of section *Paralias* [30, 31]. Our finding that *E. taurinensis* produces segetanes and no pepluanes supports the new taxonomic clasification of this species.

Cytotoxic and MDR-reversing activity of compounds **1** and **4–7** were tested on mouse T-lymphoma cells (▶ **Table 2**). It can be concluded that segetane and jatrophane diterpenes had no cytotoxic activity on the sensitive parent and the resistant MDR cells. Ingenane diterpenes **6** and **7** showed a cytotoxic effect on both cell lines. In addition, compound **7** was more potent on the resist-



▶ **Fig. 4** Efflux pump modulating activity of the isolated diterpenes **1** and **4–7** (2 µM and 20 µM), positive control verapamil (20 µM). FAR (fluorescence activity ratio) was calculated based on the following equation: FAR = (FI$_{MDR\ treated}$/FI$_{MDR\ control}$)/(FI$_{PAR\ treated}$/FI$_{PAR\ control}$). FI represents the fluorescence intensities observed for the MDR1 gene-transfected (MDR) and drug-sensitive parent (PAR) cell lines in the presence (treated) and absence (control) of the analyte.

ant cell line overexpressing ABCB1 than on the sensitive cell line (IC$_{50}$s of 62.81 µM and 82.47 µM, respectively). The most active compound was compound **6** (IC$_{50}$s of 59.83 µM and 53.35 µM, respectively), but the IC$_{50}$ values on the two cell lines were almost equal, indicating that the compound has no selectivity towards the resistant cell line.

The ABCB1-modulating activity of the compounds is presented in ▶ **Fig. 4**. Compared to the positive control verapamil, all of the compounds could inhibit the ABCB1 MDR efflux pump of the resistant mouse T-lymphoma cells, suggesting that they could be used as potential resistance modifiers. The most potent ABCB1-modulating effect was demonstrated in the case of ingenanes **6** and **7** and segetane **1** at 20 µM (FAR 59.39, 56.16, and 44.44, respectively). This is the first report of biologicaly activity of segetane-type diterpenes.

Rédei D et al. Bioactive Segetane, Ingenane, … Planta Med 2018; 84: 729–735

733

## Materials and Methods

### General experiment procedures

Optical rotations were determined in $CHCl_3$ by using a Perkin-Elmer 341 polarimeter. NMR spectra were recorded in $CDCl_3$ on a Bruker Avance DRX 500 spectrometer at 500 MHz ($^1$H) and 125 MHz ($^{13}$C). The signals of the residual solvent ($\delta_H$ 7.26, $\delta_C$ 77.2) were taken as a reference. Two-dimensional data were acquired and processed with MestReNova v6.0.2–5475 software. The energy-minimized structure was generated by Chem3D Pro 12.0.1 software using the MM2 force field method. High-resolution MS data were recorded in the positive ion mode on a Thermo Q Exactive Plus orbitrap mass spectrometer equipped with a HESI source. The resolution was over 40 000. The data were acquired and processed with Thermo Xcalibur 4.0 software. For column chromatography, polyamide (MP Polyamide, 50–160 µm; MP Biomedicals) and silica gel (TLC Silica gel 60 GF$_{254}$, 15 µm; Merck) were used. Eluted fractions were monitored on silica gel plates (TLC Silica gel 60 F$_{254}$, 0.25 mm; Merck) by spraying a stain solution of cc. $H_2SO_4$, followed by heating at 105 °C. Preparative layer chromatography was performed on normal (TLC Silica gel 60 F$_{254}$, 0.25 mm; Merck) and reversed-phase (TLC Silica gel 60 RP-18 F$_{254S}$; Merck) plates. HPLC separations were executed on a Waters Millipore instrument, with UV detection at 254 nm, on normal-phase (LiChrosper Si 100, 250 × 4 mm, 5 µm; Merck) and reversed-phase (LiChrosper RP-18, 250 × 4 mm, 5 µm; Merck) columns.

### Plant material

The whole plant (including roots) of *E. taurinensis* was collected in May 2014, in Budapest, Hungary (N 47°27′35″; E 19°3′34″), and was identified by Zoltán Barina (Department of Botany, Hungarian Natural History Museum, Budapest). A voucher specimen (No. 879) has been deposited in the Herbarium of the Department of Pharmacognosy, University of Szeged, Szeged, Hungary.

### Extraction and isolation

The fresh plant of *E. taurinensis* (1000 g) was blended, then percolated with MeOH (10 L) at room temperature. The crude extract was concentrated under reduced pressure, resuspended in aqueous MeOH, and partitioned with $CHCl_3$ (6 × 300 mL). On evaporation, the organic phase gave a residue (16.65 g), which was chromatographed on an open polyamide column with mixtures of MeOH-water (3:2 and 4:1, each 400 mL) as eluents. The fraction obtained with MeOH-water (4:1) was subjected to silica gel vacuum liquid chromatography using a gradient system of cyclohexane-ethyl acetate-EtOH (80:10:0, 60:10:0, 40:10:0, 30:10:0, 20:10:0, and 20:10:2) to yield 70 fractions (A1–70, each 10 mL). Repetitive purification of A20–30 was carried out by preparative layer chromatography on reversed-phase silica plates (RP-PLC) (acetonitrile-water 11:1) and NP-HPLC (cyclohexane-ethyl acetate-EtOH 90:15:0.2; flow rate 0.6 mL/min) to afford compounds **4** (5.4 mg), **5** (1.8 mg), and **6** (5.1 mg). Fraction A31–35 was separated by NP-PLC (cyclohexane-ethyl acetate-EtOH 25:15:1) and RP-HPLC (acetonitrile-water 6:4, flow rate 1.5 mL/min) to yield compound **2** (1.7 mg). The final fractionation of A43–50 included consecutive steps of RP-PLC (MeOH-water 10:1) and NP-HPLC (cyclohexane-ethyl acetate-EtOH 25:15:1, flow rate 1.5 mL/min), and provided compound **7** (2.1 mg). The fraction eluted from the polyamide column with MeOH-water (3:2) was transferred to a silica gel column applying a step gradient of cyclohexane-ethyl acetate-EtOH (60:10:0, 40:10:0, 30:10:0, 30:10:1, 30:20:1, and 30:20:2) to collect 80 fractions (B1–80, each 15 mL). B38–49 was separated by NP-HPLC (cyclohexane-ethyl acetate-EtOH 50:10:1, 1.5 mL/min flow rate), followed by NP-PLC (cyclohexane-ethyl acetate-EtOH 25:15:1) to furnish compound **1** (12.9 mg). Further fractionation of B50–69 was performed by means of silica gel vacuum liquid chromatography with increasing polarity of cyclohexane-$CHCl_3$-acetone (15:10:0.5, 10:20:2, 10:20:3, and 5:20:5) solvent systems (C1–51, each 5 mL). C7 was submitted to RP-PLC separation (acetonitrile-water 3:1) to afford compound **3** (12.1 mg).

### Cell lines

The L5178Y mouse T-lymphoma cells (PAR) (ECACC Cat. No. 87111908, obtained from the FDA) were transfected with pHa MDR1/A retrovirus, as previously described by Cornwell et al. [32]. The ABCB1-expressing cell line L5178Y (MDR) was selected by culturing the infected cells with colchicine. L5178Y (parent) mouse T-cell lymphoma cells and the L5178Y human ABCB1-transfected subline were cultured in McCoy's 5A medium (Sigma-Aldrich) supplemented with 10% heat-inactivated horse serum (Sigma-Aldrich), 200 mM L-glutamine (Sigma-Aldrich), and a penicillin-streptomycin (Sigma-Aldrich) mixture in concentrations of 100 U/L and 10 mg/L, respectively.

### Assay for cytotoxic effect

The cytotoxicity assay was performed according to the protocol described by Domínguez-Álvarez et al. [33]. The effects of increasing concentrations of compounds on cell growth were tested in 96-well flat-bottomed microtiter plates. The compounds were dissolved in DMSO for the experiments. Doxorubicin (purity 98–102%; Sigma-Aldrich) was applied as a positive control. The final concentration of DMSO (solvent control) was 1%. The same DMSO concentration was used for the control. The samples were diluted in a volume of 100 µL medium. Then, $2 \times 10^4$ cells in 100 µL of medium were added to each well, with the exception of the medium control wells. The culture plates were incubated at 37 °C for 72 h. At the end of the incubation period, 20 µL of thiazolyl blue tetrazolium bromide (Sigma-Aldrich) solution (from a 5-mg/mL stock) were added to each well. After incubation at 37 °C for 4 h, 100 µL of sodium dodecyl sulfate (Sigma-Aldrich) solution (10% in 0.01 M HCl) were added to each well and the plates were further incubated at 37 °C overnight. Cell growth was determined by measuring the OD at 550 nm (ref. 630 nm) with a Multiscan EX ELISA reader (Thermo Labsystems). Inhibition of the cell growth was determined according to the formula:

$$100 - \frac{OD_{sample} - OD_{medium\ control}}{OD_{cell\ control} - OD_{medium\ control}} \times 100$$

Results are expressed in terms of IC$_{50}$, defined as the inhibitory dose that reduces the growth of the cells exposed to the tested

734

Rédei D et al. Bioactive Segetane, Ingenane… Planta Med 2018; 84: 729–735

compound by 50%. The data were evaluated using dose-response curves and nonlinear regression. The IC$_{50}$ values were calculated using GraphPad Prism 6 software. Data represent the mean and confidence interval (CI) of three independent experiments.

## Rhodamine 123 accumulation assay by flow cytometry

First, the inhibition of ABCB1 by the tested compounds was evaluated using flow cytometry measuring the retention of R123 by ABCB1 (P-glycoprotein) in MDR mouse T-lymphoma cells overexpressing the ABCB1 protein. The cell number of L5178Y MDR and L5178Y parental cell lines was adjusted to $2 \times 10^6$ cells/mL, resuspended in serum-free McCoy's 5A medium, and distributed in 0.5 mL aliquots into Eppendorf centrifuge tubes. The tested compounds were added at 2 and 20 μM concentrations, and the samples were incubated for 10 min at room temperature. Verapamil (purity ≥ 99%; Sigma-Aldrich) was applied as a positive control. DMSO at 2% was applied as the solvent control. Next, 10 μL (5.2 μM final concentration) of the fluorochrome and ABCB1 substrate R123 (Sigma-Aldrich) were added to the samples, and the cells were incubated for a further 20 min at 37 °C, washed twice, and resuspended in 0.5 mL PBS for analysis. The results obtained from a representative flow cytometry experiment measuring 10 000 individual cells of the population were evaluated using a CyFlow flow cytometer (Partec). The percentage of mean fluorescence intensity was calculated for the treated MDR cells as compared to the untreated cells. A FAR was calculated based on the following equation that relates the measured fluorescence values:

$$\text{FAR} = \frac{\text{Fl}_{\text{MDR treated}} \; / \; \text{Fl}_{\text{MDR control}}}{\text{Fl}_{\text{PAR treated}} \; / \; \text{Fl}_{\text{PAR control}}}$$

Fl represents the fluorescence intensities observed for the MDR1 gene-transfected (MDR) and drug-sensitive parent (PAR) cell lines in the presence (treated) and absence (control) of the analyte [34].

*6,14-Diacetoxy-5-(2-acetoxyacetoxy)-3-benzoyloxy-15-hydroxy-9-oxo-segetane (1)*: White solid, $[\alpha]_D^{25}$ + 22 (c = 0.1, CHCl$_3$), UV (MeOH) $\lambda_{max}$ (log $\varepsilon$) 202 (3.94), 231 (4.08), 274 (2.97) nm, $^1$H NMR (500 MHz, CDCl$_3$) and $^{13}$C NMR (125 MHz, CDCl$_3$) data, see in ▶ **Table 1**. HRESIMS (positive ion mode): m/z 674.3180 [M + NH$_4$]$^+$ (calcd. for C$_{35}$H$_{48}$O$_{12}$N 674.3177, $\Delta$ = − 0.3 mmu), m/z 679.2729 [M + Na]$^+$ (calcd. for C$_{35}$H$_{44}$O$_{12}$Na 679.2731, $\Delta$ = + 0.2 mmu), 597.2701 [M + H − CH$_3$COOH]$^+$ (calcd. for C$_{33}$H$_{41}$O$_{10}$ 597.2700, $\Delta$ = − 0.1 mmu).

*5,9-Diacetoxy-3-cinnamoyloxy-15-hydroxy-14-oxo-jatropha-6(17),11E-diene (2)*: White solid, $[\alpha]_D^{25}$ + 20 (c = 0.2, CHCl$_3$), UV (MeOH) $\lambda_{max}$ (log $\varepsilon$) 218 (3.89), 222 (3.90), 279 (3.94) nm, $^1$H NMR (500 MHz, CDCl$_3$) and $^{13}$C NMR (125 MHz, CDCl$_3$) data, see in ▶ **Table 1**. HRESIMS (positive ion mode): m/z 589.2773 [M + Na]$^+$ (calcd. for C$_{33}$H$_{42}$O$_8$Na 589.2777, $\Delta$ = + 0.4 mmu), 507.2744 [M + H − CH$_3$COOH]$^+$ (calcd. for C$_{31}$H$_{39}$O$_6$ 507.2747, $\Delta$ = + 0.3 mmu).

## Supporting information

HRMS and NMR spectra of **1** and **2**, flow cytometric charts of **1**, **4**–**7**, and cytotoxicity dose-response curves of **6** and **7** are available as Supporting Information.

## Conflict of Interest

The authors declare no conflict of interest.

## References

[1] The Plant List (2013). Version 1.1. Available at http://www.theplantlist.org/. Accessed January 1, 2018

[2] Evans FJ, Taylor SE. Pro-inflammatory, tumour-promoting and anti-tumour Diterpenes of the Plant Families Euphorbiaceae and Thymelaeaceae. In: Herz W, Grisebach H, Kirby GW, eds. Progress in the Chemistry of organic natural Products, Vol. 44. Vienna: Springer; 1983: 1–99

[3] Vasas A, Hohmann J. *Euphorbia* diterpenes: isolation, structure, biological activity, and synthesis (2008–2012). Chem Rev 2014; 114: 8579–8612

[4] Boyle GM, D'Souza MMA, Pierce CJ, Adams RA, Cantor AS, Johns JP, Maslovskaya L, Gordon VA, Reddell PW, Parsons PG. Intra-lesional injection of the novel PKC activator EBC-46 rapidly ablates tumors in mouse models. PLoS One 2014; 9: e108887

[5] Williams SA, Chen LF, Kwon H, Fenard D, Bisgrove D, Verdin E, Greene WC. Prostratin antagonizes HIV latency by activating NF-kappaB. J Biol Chem 2004; 279: 42008–42017

[6] Lai W, Huang L, Zhu L, Ferrari G, Chan C, Li W, Lee KH, Chen CH. Gnidimacrin, a potent anti-HIV diterpene, can eliminate latent HIV-1 *ex vivo* by activation of protein kinase C *β*. J Med Chem 2015; 58: 8638–8646

[7] Vasas A, Rédei D, Csupor D, Molnár J, Hohmann J. Diterpenes from European *Euphorbia* species serving as prototypes for natural-product-based drug discovery. Eur J Org Chem 2012; 2012: 5115–5130

[8] Kissin I, Szallasi A. Therapeutic targeting of TRPV1 by resiniferatoxin, from preclinical studies to clinical trials. Curr Top Med Chem 2011; 11: 2159–2170

[9] Resiniferatoxin to treat severe pain associated with advanced cancer. Available at https://clinicaltrials.gov/show/NCT00804154. Accessed January 1, 2018

[10] Study to evaluate safety and MTD of epidural resiniferatoxin injection for treatment of intractable cancer pain. Available at https://clinicaltrials.gov/ct2/show/NCT03226574. Accessed January 1, 2018

[11] Hohmann J, Molnár J, Rédei D, Evanics F, Forgo P, Kálmán A, Argay G, Szabó P. Discovery and biological evaluation of a new family of potent modulators of multidrug resistance: reversal of multidrug resistance of mouse lymphoma cells by new natural jatrophane diterpenoids isolated from *Euphorbia* species. J Med Chem 2002; 45: 2425–2431

[12] Lanzotti V, Barile E, Scambia G, Ferlini C. Cyparissins A and B, jatrophane diterpenes from *Euphorbia cyparissias* as Pgp inhibitors and cytotoxic agents against ovarian cancer cell lines. Fitoterapia 2015; 104: 75–79

[13] Wang HY, Wang JS, Wei DD, Wang XB, Luo J, Yang MH, Kong LY. Bioactivity-guided isolation of antiproliferative diterpenoids from *Euphorbia kansui*. Phytother Res 2012; 26: 853–859

Rédei D et al. Bioactive Segetane, Ingenane, … Planta Med 2018; 84: 729–735

735

[14] Mongkolvisut W, Sutthivaiyakit S. Antimalarial and antituberculous poly-O-acylated jatrophane diterpenoids from *Pedilanthus tithymaloides*. J Nat Prod 2007; 70: 1434–1438

[15] Nothias-Scaglia LF, Retailleau P, Pannecouque C, Neyts J, Dumontet V, Roussi F, Leyssen P, Costa J, Litaudon M. Jatrophane diterpenes as inhibitors of chikungunya virus replication: structure-activity relationship and discovery of a potent lead. J Nat Prod 2014; 77: 1505–1512

[16] Bedoya LM, Márquez N, Martínez N, Guitérrez-Eisman S, Alvarez A, Calzado MA, Rojas JM, Appendino G, Muñoz E, Alcamí J. SJ23B, a jatrophane diterpene activates classical PKCs and displays strong activity against HIV *in vitro*. Biochem Pharmacol 2009; 77: 965–978

[17] Ferreira RJ, dos Santos DJ, Ferreira MJ, Guedes RC. Toward a better pharmacophore description of P-glycoprotein modulators, based on macrocyclic diterpenes from *Euphorbia* species. J Chem Inf Model 2011; 51: 1315–1324

[18] Wiśniewski J, Wesołowska O, Środa-Pomianek K, Paprocka M, Bielawska-Pohl A, Krawczenko A, Duarte N, Ferreira MJ, Duś D, Michalak K. *Euphorbia* species-derived diterpenes and coumarins as multidrug resistance modulators in human colon carcinoma cells. Anticancer Res 2016; 36: 2259–2264

[19] Reis MA, Ahmed OB, Spengler G, Molnár J, Lage H, Ferreira MJ. Jatrophane diterpenes and cancer multidrug resistance – ABCB1 efflux modulation and selective cell death induction. Phytomedicine 2016; 23: 968–978

[20] Smith AR, Tutin TG. 7. Euphorbia L. In: Tutin TG, Heywood VH, Burges NA, Moore DM, Valentine DH, Walters SM, Webb DA, eds. Flora Europaea, Vol. 2. Cambridge: Cambridge University Press; 1968: 213–226

[21] Abdelgaleil SA, Kassem SM, Doe M, Baba M, Nakatani M. Diterpenoids from *Euphorbia paralias*. Phytochemistry 2001; 58: 1135–1139

[22] Jakupovic J, Jeske F, Morgenstern F, Tsichritzis F, Marco JA, Berendsohn W. Diterpenes from *Euphorbia segetalis*. Phytochemistry 1998; 47: 1583–1600

[23] Corea G, Fattorusso C, Fattorusso E, Lanzotti V. Amygdaloidins A–L, twelve new 13 α-OH jatrophane diterpenes from *Euphorbia amygdaloides* L. Tetrahedron 2005; 61: 4485–4494

[24] Öksüz S, Gürek F, Yang SW, Lin LZ, Cordell GA, Pezzuto JM, Wagner H, Lotter H. Paralinones A and B, novel diterpene esters from *Euphorbia paralias*. Tetrahedron 1997; 53: 3215–3222

[25] Gotta H, Adolf W, Opferkuch HJ, Hecker E. On the active principles of the Euphorbiaceae, IX a ingenane type diterpene esters from five *Euphorbia* species. Z Naturforsch B 1984; 39: 683–694

[26] Jakupovic J, Morgenstern T, Marco JA, Berendsohn W. Diterpenes from *Euphorbia paralias*. Phytochemistry 1998; 47: 1611–1619

[27] Madureira AM, Gyémánt N, Ascenso JR, Abreu PM, Molnar J, Ferreira MJ. Euphoportlandols A and B, tetracylic diterpene polyesters from *Euphorbia portlandica* and their anti-MDR effects in cancer cells. J Nat Prod 2006; 69: 950–953

[28] Barile E, Lanzotti V. Biogenetical related highly oxygenated macrocyclic diterpenes from sea spurge *Euphorbia paralias*. Org Lett 2007; 9: 3603–3606

[29] Wan LS, Shao LD, Fu L, Xu J, Zhu GL, Peng XR, Li XN, Li Y, Qui MH. One-step semisynthesis of a segetane diterpenoid from a jatrophane precursor via a Diels-Alder reaction. Org Lett 2016; 18: 496–499

[30] Riina R, Peirson JA, Geltman DV, Molero J, Frajman B, Pahlevani A, Barres L, Morawetz JJ, Salmaki Y, Zarre S, Kryukov A, Bruyns P, Berry PE. A worldwide molecular phylogeny and classification of the leafy spurges, *Euphorbia* subgenus *Esula* (Euphorbiaceae). Taxon 2013; 62: 316–342

[31] Shavarda AL, Geltman DV. Skeleton types of diterpenoids and the system of genus *Euphorbia* (Euphorbiaceae). Rastitelnye Resursy 2017; 53: 163–195

[32] Cornwell MM, Pastan I, Gottesman MM. Certain calcium channel blockers bind specifically to multidrug-resistant human KB carcinoma membrane vesicles and inhibit drug binding to P-glycoprotein. J Biol Chem 1987; 262: 2166–2170

[33] Domínguez-Álvarez E, Gajdács M, Spengler G, Palop JA, Marć MA, Kieć-Kononowicz K, Amaral L, Molnár J, Jacob C, Handzlik J, Sanmartín C. Identification of selenocompounds with promising properties to reverse cancer multidrug resistance. Bioorg Med Chem Lett 2016; 26: 2821–2824

[34] Molnár J, Gyémánt N, Mucsi I, Molnár A, Szabó M, Körtvélyesi T, Varga A, Molnár P, Tóth G. Modulation of multidrug resistance and apoptosis of cancer cells by selected carotenoids. In Vivo 2004; 18: 237–244